J. Cell. Mol. Med. Vol 13, No 2, 2009 pp. 295-308

A distinct type of cell in myocardium: interstitial Cajal-like cells (ICLCs)

S. Kostin [a, *], L. M. Popescu [b, c, *]

[a] *Max-Planck Institute for Heart and Lung Research (W.C. Kerckhoff Institute), Bad Nauheim, Germany*
[b] *'Victor Babes' National Institute of Pathology, Bucharest, Romania*
[c] *Department of Cellular and Molecular Medicine, 'Carol Davila' University of Medicine and Pharmacy, Bucharest, Romania*

Received: November 30, 2008; Accepted: December 21, 2008

Abstract

The existence of a novel type of interstitial cells in the heart, interstitial Cajal-like cells (ICLCs), had been described for the first time in 2005. Their identification was mainly based on ultrastructural criteria: very long (tens up to hundreds of micrometres) and moniliform prolongations, which are extremely thin (less than 0.2 μm), below the resolving power of light microscopy. Myocardial ICLCs were also identified by methylene-blue vital staining, silver impregnation, and immunoreactivity for CD 34, vimentin, CD117/c-kit, etc. Although a series of studies provided evidence for the existence of ICLCs in human atria and rat ventricles, further investigations in other laboratories, using additional techniques, are required to substantiate the consistency of these findings. Here we provide further evidence for the existence of ICLCs in human and mammalian hearts (by transmission and scanning electron microscopy, as well as confocal laser scanning microscopy). Noteworthy, we confirm that ICLCs communicate with neighbouring cells *via* shedding (micro)vesicles. Although these so-called ICLCs represent a distinct type of cells, different from classical interstitial cells of Cajal, or fibroblasts, their role(s) in myocardium remain(s) to be established. Several hypotheses are proposed: (*i*) adult stromal (mesenchymal) stem cells, which might participate in cardiac repair/remodelling; (*ii*) intercellular signalling (*e.g. via* shedding microvesicles); (*iii*) chemo-mechanical transducers and (*iv*) players in pacemaking and/or arrhytmogenesis, and so on.

Keywords: interstial Cajal-like cells (ICLCs) • myocardium • adult mesenchymal stem cells • cardiac repair • shedding (micro)vesicles • arrhytmogenesis • vimentin • c-kit • CD34 • chemo-mechanical transducers

Introduction

Interstitial cells of Cajal (ICC) have extensively been characterized in the gastrointestinal tract (for reviews, see [1–6]). However, recently questions were raised about the presence of ICC outside the musculature of the gastrointestinal tract [7], and such cells were named interstitial Cajal-like cells (ICLCs) [8–11]. ICLCs have been identified in numerous organs: pancreas [12], gallbladder [13–15], urinary tract [16–22], myometrium [11, 23–28], fallopian tube [11, 29, 30], mammary gland [8], placenta [31], prostate [32] and mesentery [33], including the vasculature [34–38]. Noteworthy, very recently Faussone-Pellegrini and co-workers [39], based on immunoelectron microscopy, identified ICLCs in the gastrointestinal muscle of human beings, beyond the 'classical' ICC.

The very first demonstration of ICLC presence in the heart had been reported by Hinescu and Popescu in 2005 [9]. Despite a series of papers that followed [10, 40–43] showing the existence of ICLCs in various parts of the heart, more studies are certainly needed, especially using other techniques to substantiate independently the consistency of these findings. Therefore, the present study aims to investigate the nanometre details of ICLCs in human and rat myocardium using transmission (TEM) and scanning electron microscopy (SEM) as well as confocal laser scanning microscopy (CLSM).

Material and methods

Experimental animals

Adult rat hearts were obtained from five Wistar rats (90 days old). The animals were deeply anesthetized with pentobarbital (20 mg/kg body weight).

*Correspondence to: Dr. Sawa KOSTIN, M.D., Ph.D.,
Max-Planck-Institute for Heart and Lung Research (W.C. Kerckhoff Institute), Parkstrasse 1, 61231 Bad Nauheim, Germany.
Tel.: +49 6032 705 420; Fax: +49 6032 705 458
E-mail: sawa.kostin@mpi-bn.mpg.de

L.M. POPESCU, M.D., Ph.D.,
Department of Cellular and Molecular Medicine,
"Carol Davila" University of Medicine and Pharmacy,
P.O. Box 35-29, Bucharest 35, Romania.
E-mail: LMP@jcmm.org

doi:10.1111/j.1582-4934.2008.00668.x

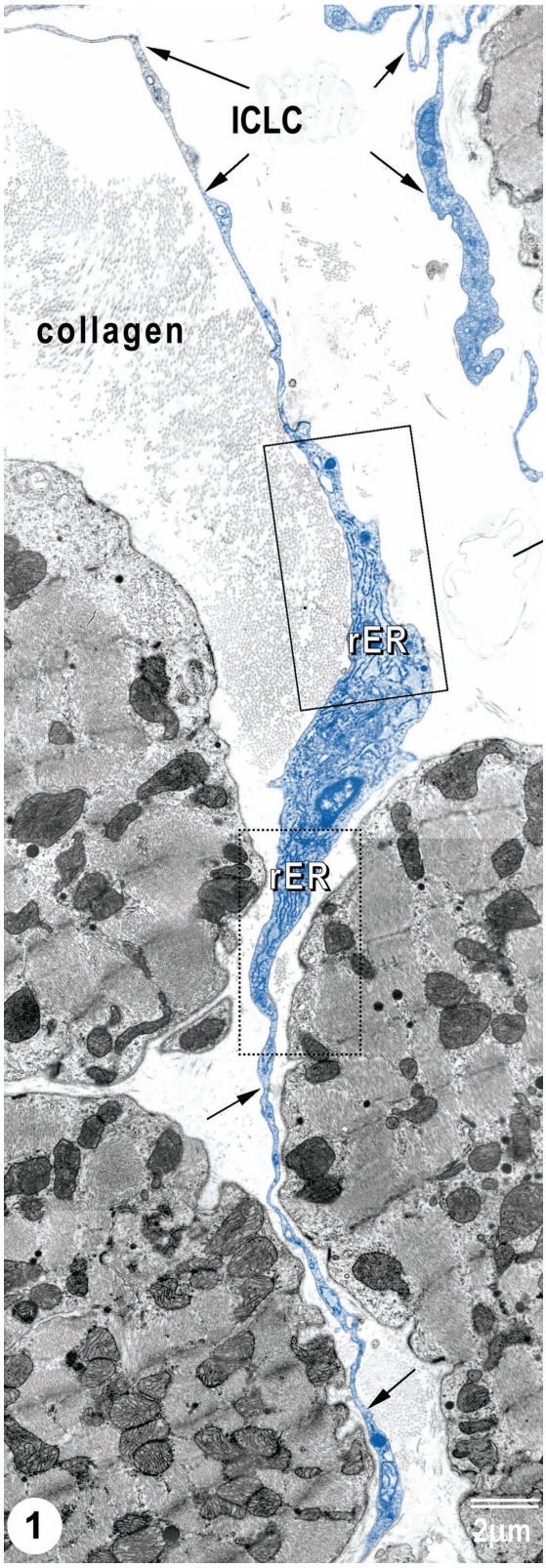

The abdominal aorta was cannulated and the right atrium was opened. After 2 min. of retrograde myocardial perfusion through the abdominal catheter (80 mmHg perfusion pressure) with oxygen-saturated Tyrode's solution, hearts were perfused for 15 min. with 2% glutaraldehyde in 0.1 mmol natrium cacodylate for TEM as described, or with 2% paraformaldehyde in 0.1 mmol/l phosphate-buffered saline (PBS) for immunohistochemistry. The institutional Ethical Committee approved the study.

Human myocardium

We have investigated human myocardium from three donor hearts that for technical reasons were not used for heart transplantation. Specimens were either fixed in 4% freshly prepared paraformaldehyde, cryoprotected with 20% sucrose, quick-frozen in methylbutane at –130°C and stored at –80°C, or were fixed in 3% glutaraldehyde. The institutional Ethical Committee approved the study.

Transmission electron microscopy

Specimens pre-fixed in glutaraldehyde were post-fixed in 2% osmium tetroxide for 1 hr. After dehydration in graded concentrations of alcohol and propylene oxide, they were embedded in Epon, following routine procedures. Semithin (1 μm) sections were stained with toluidine blue and viewed in a Leica DM microscope (Wetzlar, Germany). Ultrathin sections were stained with uranyl acetate and lead citrate, and viewed and photographically recorded under a Philips CM 10 electron microscope (Eindhoven, The Netherlands) as described.

Scanning electron microscopy

Glutaraldehyde pre-fixed specimens were washed in 0.1 mmol natrium cacodylate buffer (pH 7.4) and immersed in 6 N NaOH for 10–15 min. at 60°C to digest collagen fibres and basement membrane as previously described [44]. The specimens were washed thoroughly in PBS and post-fixed in 1% osmium tetroxide for 1 hr. They were finally dehydrated in graded concentrations of alcohol, dried by the tbutylalcohol freeze drying method, coated with gold using an ioncoater and examined in a Hitachi S-800 electron microscope as described previously [45].

Immunohistochemistry and confocal laser scanning microscopy

Frozen tissue cryosections (10 μm thick) were placed on gelatin-coated slides and incubated for 15 min. with 100 mmol glycine and 0.1% carboxylated bovine serum albumin (Aurion, Wageningen, The Netherlands) in PBS, pH 7.4. Then the cryosections were incubated overnight with the primary antibody against vimentin (clone V9; Sigma, St Louis, MO, USA) in a moist

Fig. 1 TEM image of ICLCs (rat) in the right atrial interstitium. ICLCs are indicated by arrows. Note the characteristic aspects of ICLC processes: very long and very thin cellular elongations, with uneven calibre (moniliform aspect). Insets show portions of ICLC cell body, containing (abundant) rough endoplasmic reticulum.

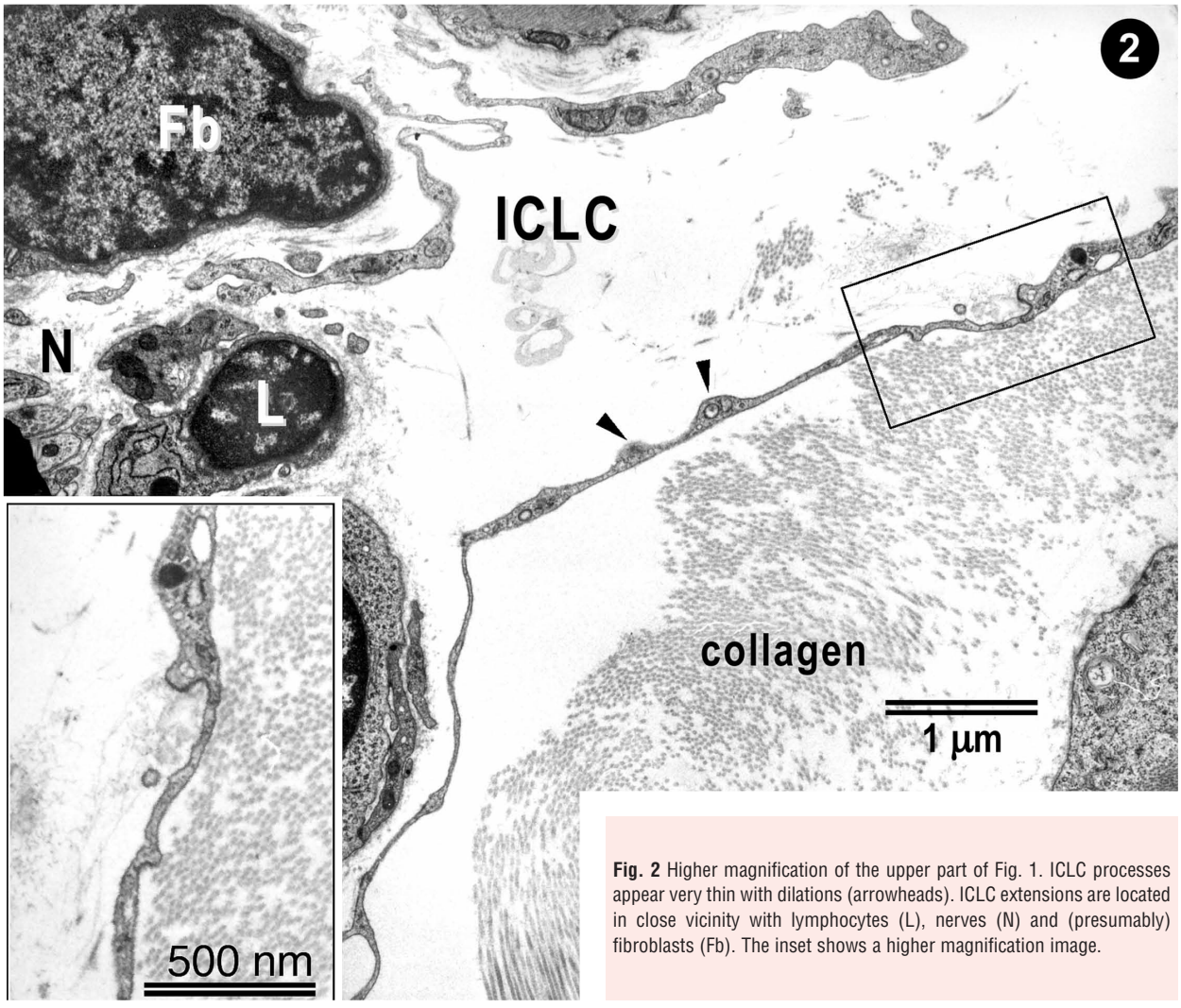

Fig. 2 Higher magnification of the upper part of Fig. 1. ICLC processes appear very thin with dilations (arrowheads). ICLC extensions are located in close vicinity with lymphocytes (L), nerves (N) and (presumably) fibroblasts (Fb). The inset shows a higher magnification image.

chamber. After washing in PBS, the preparations were incubated with biotinylated donkey antimouse IgG followed by streptavidin-Cy-2 (Biotrend, Cologne, Germany). The nuclei were stained with 0.002% 7-aminoactinomycin D (Molecular Probes, Carlsbad, CA, USA). Omission of the primary antibody served as a negative control.

The immunolabelled sections were examined with a Leica TCN-NT laser microscope, equipped with argon/krypton and helium/neon laser. Series of confocal sections were taken through the depth of the tissue samples at 0.5-μm intervals. In order to improve image quality and to obtain a high signal/noise ratio each image from the series was signal averaged. After data acquisition, the images were transferred to a Silicon Graphics Indy or Octane workstations (Silicon Graphics, Sunnyvale, CA, USA) for image restoration and reconstruction using Imaris, the multi-channel image processing software (Bitplane, Zürich, Switzerland). The principles of this method and numerous images obtained with this technique have been previously published [46, 47]. In double-labelling experiments, cryosections were incubated overnight with the primary polyclonal antibody against c-kit (Dako, Glostrup, Denmark) followed by donkey anti-rabbit IgG coupled with Cy2 (Dianova, Hamburg, Germany). After repeated washes in PBS, the preparations were incubated with antivimentin antibodies directly coupled with Cy3. Myofibrils were stained for F-actin with Alexa 633-conjugated phalloidin. The nuclei were stained with 4′,6-diamidino-2-phenylindole (DAPI) (Molecular Probes). All preparations were mounted in Mowiol (Hoechst, Frankfurt, Germany). Classical immunocytochemistry was performed on fomalin-fixed, paraffin-embedded tissue sections by the avidin-biotin peroxidase complex method, as previously reported [10]. The primary antibodies used were: CD34 – monoclonal, 1: 100, clone QBEND 10 (Biogenex, San Ramon, CA, USA) and vimentin, monoclonal, 1: 100, clone V-9 (Biogenex).

Results

Figure 1 shows the general aspect ('silhouette') of a typical fusiform cell body with two very long (tens of micrometers) cytoplasmic prolongations placed between cardiomyocytes. Note the characteristic appearance of ICLC processes: unequal thickness,

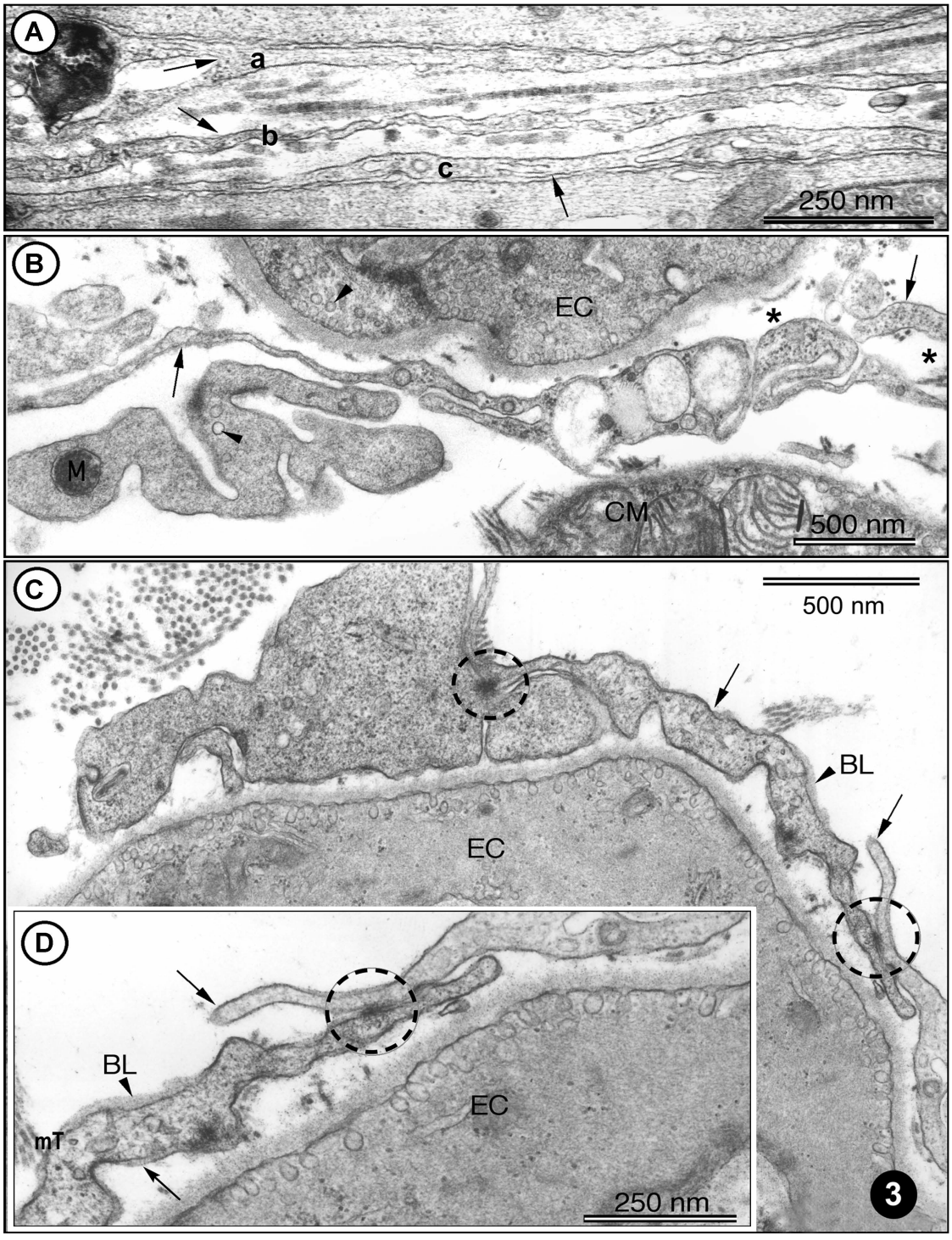

Fig. 3 (**A**)–(**D**) TEM images of rat left ventricular myocardium. (**A**) Three ICLC processes (arrows: a, b, c) are located in the myocardial interstitium. Note the cross-striated pattern of collagen fibrils (in the middle part). (**B**) A typical example of ICLC processes (arrows) located in vicinity of endothelial cells (EC) and cardiomyocytes. The presence of caveolae (arrowheads) is a typical feature of ICLCs and ECs. Note the cross-section of intermediate

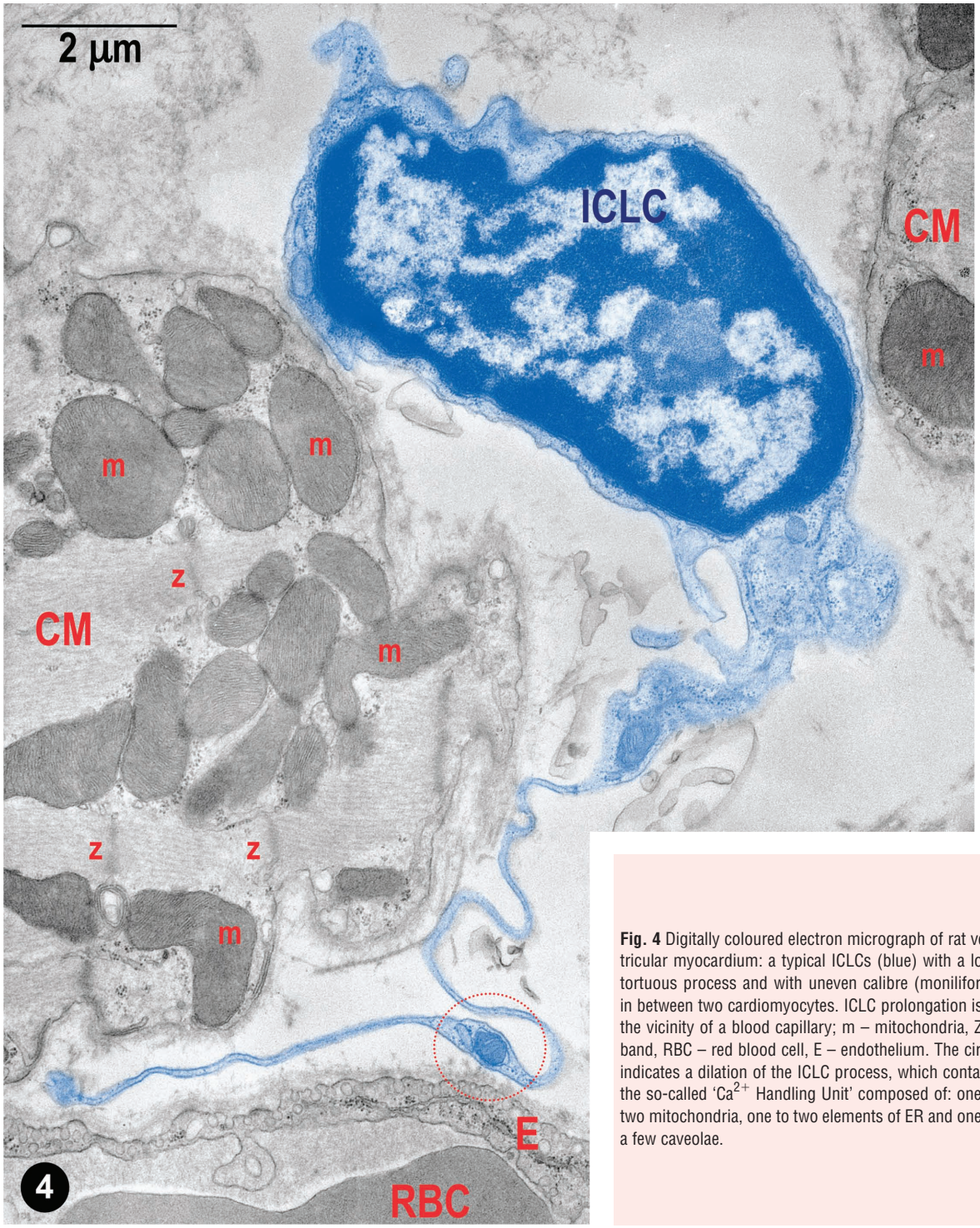

Fig. 4 Digitally coloured electron micrograph of rat ventricular myocardium: a typical ICLCs (blue) with a long tortuous process and with uneven calibre (moniliform) in between two cardiomyocytes. ICLC prolongation is in the vicinity of a blood capillary; m – mitochondria, Z–Z band, RBC – red blood cell, E – endothelium. The circle indicates a dilation of the ICLC process, which contains the so-called 'Ca^{2+} Handling Unit' composed of: one to two mitochondria, one to two elements of ER and one or a few caveolae.

filaments (asterisk) inside ICLC processes. (**C**) ICLCs (arrows) located in close vicinity of endothelial cells (EC). Cell-to-cell contacts of ICLCs are indicated with circles. Note the presence of the basal lamina (BL, arrowhead), which can occasionally be observed in ICLCs. (**D**) Higher magnification of the right part of (**C**) showing jonctional complexes (circle) between two ICLCs, indicated with arrows. BL – basal lamina. Cross-sectioned microtubules (mT) can be seen in ICLC processes.

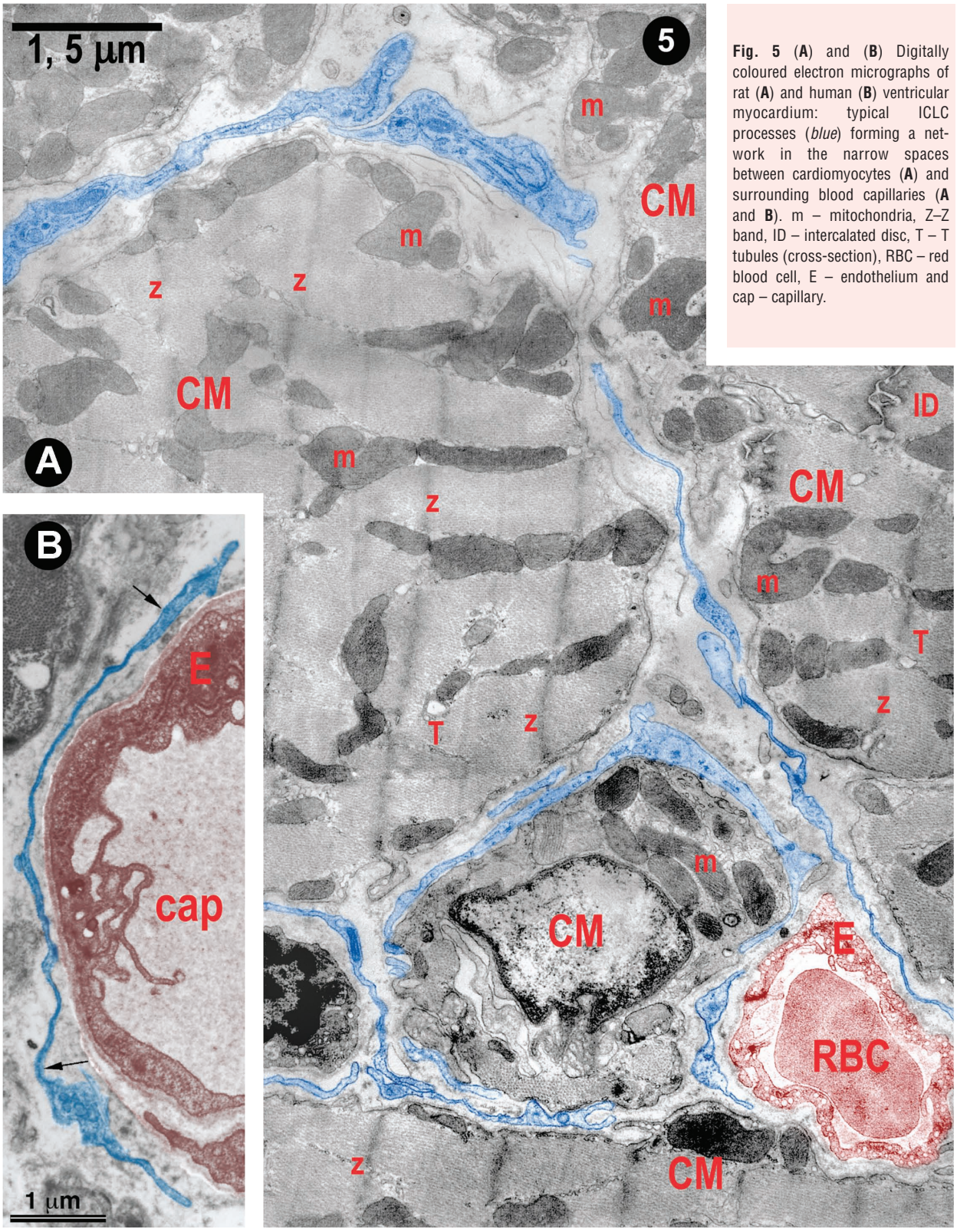

Fig. 5 (**A**) and (**B**) Digitally coloured electron micrographs of rat (**A**) and human (**B**) ventricular myocardium: typical ICLC processes (*blue*) forming a network in the narrow spaces between cardiomyocytes (**A**) and surrounding blood capillaries (**A** and **B**). m – mitochondria, Z–Z band, ID – intercalated disc, T – T tubules (cross-section), RBC – red blood cell, E – endothelium and cap – capillary.

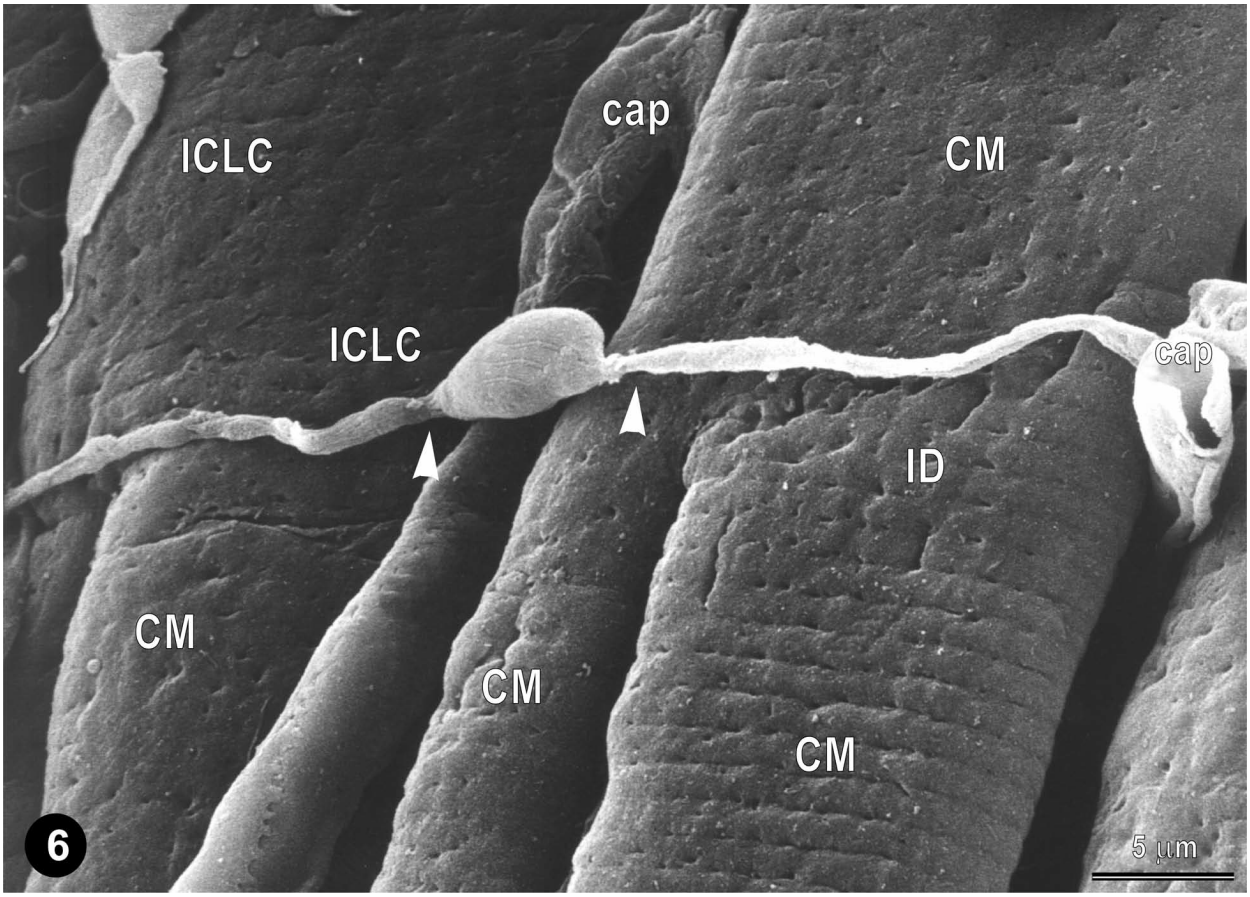

Fig. 6 Representative scanning electron micrograph (monkey left ventricular myocardium) showing a typical ICLC located across the cardiomyocytes. Another (possible) ICLC appears located along the cardiomyocytes (upper left). The three-dimensional vision reveals close interconnections of ICLCs with cardiomyocytes and capillaries (cap); compare with Fig. 5. Note that ICLC processes begin from the cell body abruptly, as very thin prolongations (arrow heads); ID.

sudden narrowing after coming off the cell body and dilated portions alternating with slender segments. Thus, the moniliform aspect of ICLC processes is evident. The dilated portions contain usually: caveolae, elements of endoplasmic reticulum and/or mitochondria. Fragments of tortuous ICLC processes (intersected by the plane of the ultrathin section) appear in Fig. 1, right upper part.

Higher magnifications (Fig. 2) provide additional evidence, with knobs along ICLC processes. Noteworthy, ICLC processes are located in the vicinity of nerve fibres, immunocompetent cells, and fibroblasts, eventually.

Figure 3 shows some morphological characteristics details of ICLC processes. It is obvious (Fig. 3A) that the thickness of the three ICLC processes (a–c) is far below the resolving power of light microscope (0.2 μm) and therefore, such 'structures' of 40–50 nm diameter are visible only by electron microscopy. This may explain the fact that, in order to be constantly observed, ICLC processes had to "wait" for the technology of high-resolution TEM. It is to be mentioned that Fig. 3 presents labyrinthic network of ICLC processes. Typically, ICLC processes show caveolae, short membrane associated dense bands, and relatively numerous close appositions.

Figures 4 and 5 present the location of ICLC convoluted processes between cardiac miocytes and blood capillaries. Moreover, Fig. 5A shows clearly that the tentacular ICLC processes may surround (completely) other cardiac myocytes, or blood capillaries, or both. Hereby, ICLC processes suggest the existence of a bi(three)-dimensional network. This impression is strengthened by the scanning electron micrograph in Fig. 6. The three-dimensional image shows, unequivocally, the silhouette of a very long, slender bipolar ICLCs, which has close contacts with at least two blood capillaries and at least four ICLCs. Compare the three dimensional of Fig. 6 with the bi-dimensional view of Fig. 5. Another ICLC (Fig. 6), upper left corner, is located parallel to cardiomiocytes and blood vessels.

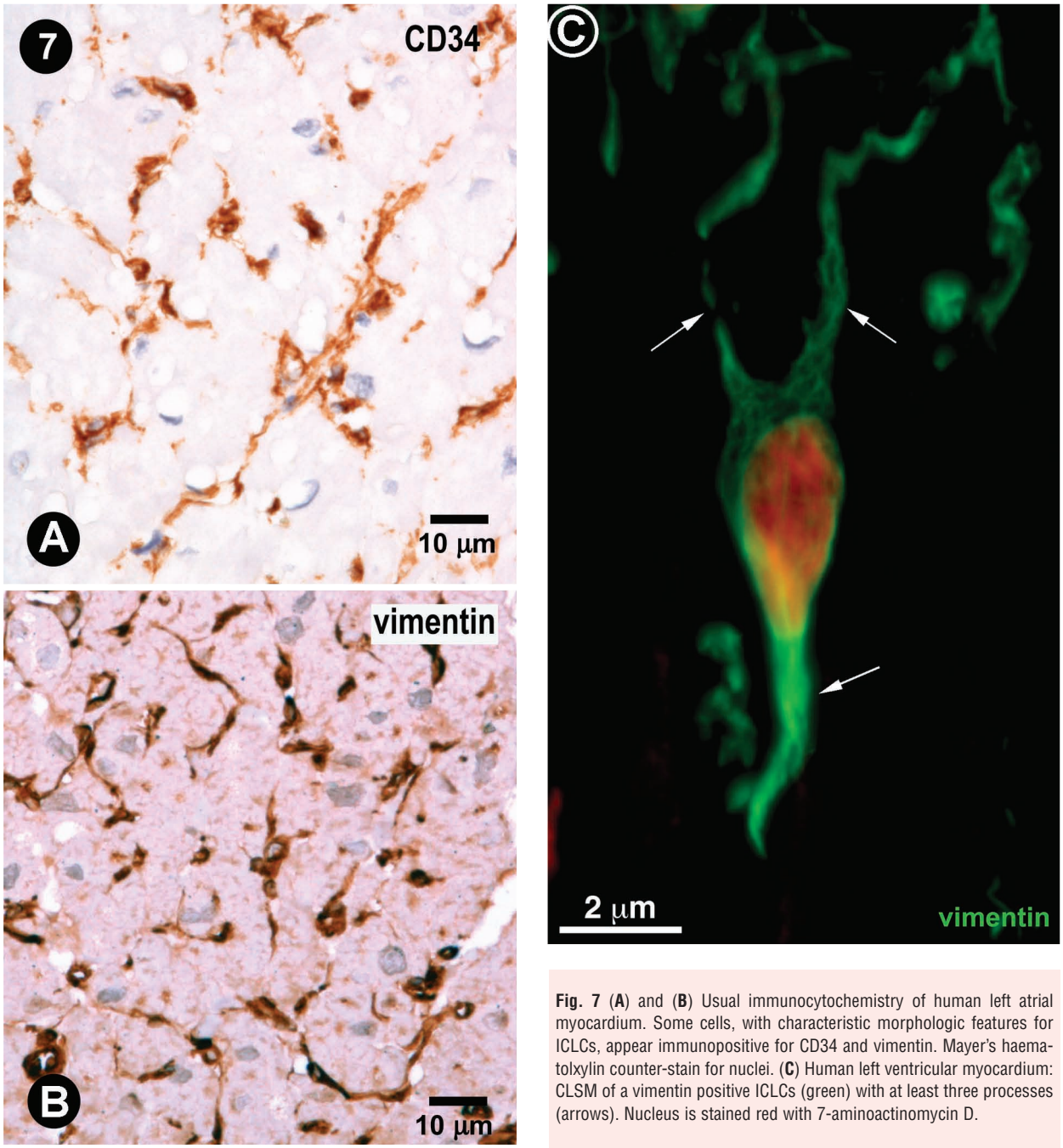

Fig. 7 (**A**) and (**B**) Usual immunocytochemistry of human left atrial myocardium. Some cells, with characteristic morphologic features for ICLCs, appear immunopositive for CD34 and vimentin. Mayer's haematolxylin counter-stain for nuclei. (**C**) Human left ventricular myocardium: CLSM of a vimentin positive ICLCs (green) with at least three processes (arrows). Nucleus is stained red with 7-aminoactinomycin D.

Currently, there is not generally accepted panel of antibodies for ICLC immunophenotyping. However, customary markers include CD117/c-kit, CD34, vimentin, α smooth muscle actin, etc. We previously reported that polyclonal antibodies used against CD117/c-kit resulted in a weakly and inconstantly positive immunostaining of ICLCs [10, 40]. Thus, we tested the presence of CD34 and vimentin antigens. The images of Fig. 7A and B suggest that, from the point of view of usual light-microscope immunohistochemistry, most of $CD34^{+}$ cells and vimentin positive cells might be superposed. A network-like distribution of such ICLCs seems in accordance with TEM data. Figure 7C obtained by CLSM reveals a vimentin positive ICLCs. Vimentin localization is predominant along the processes, as previously reported in cell culture [29].

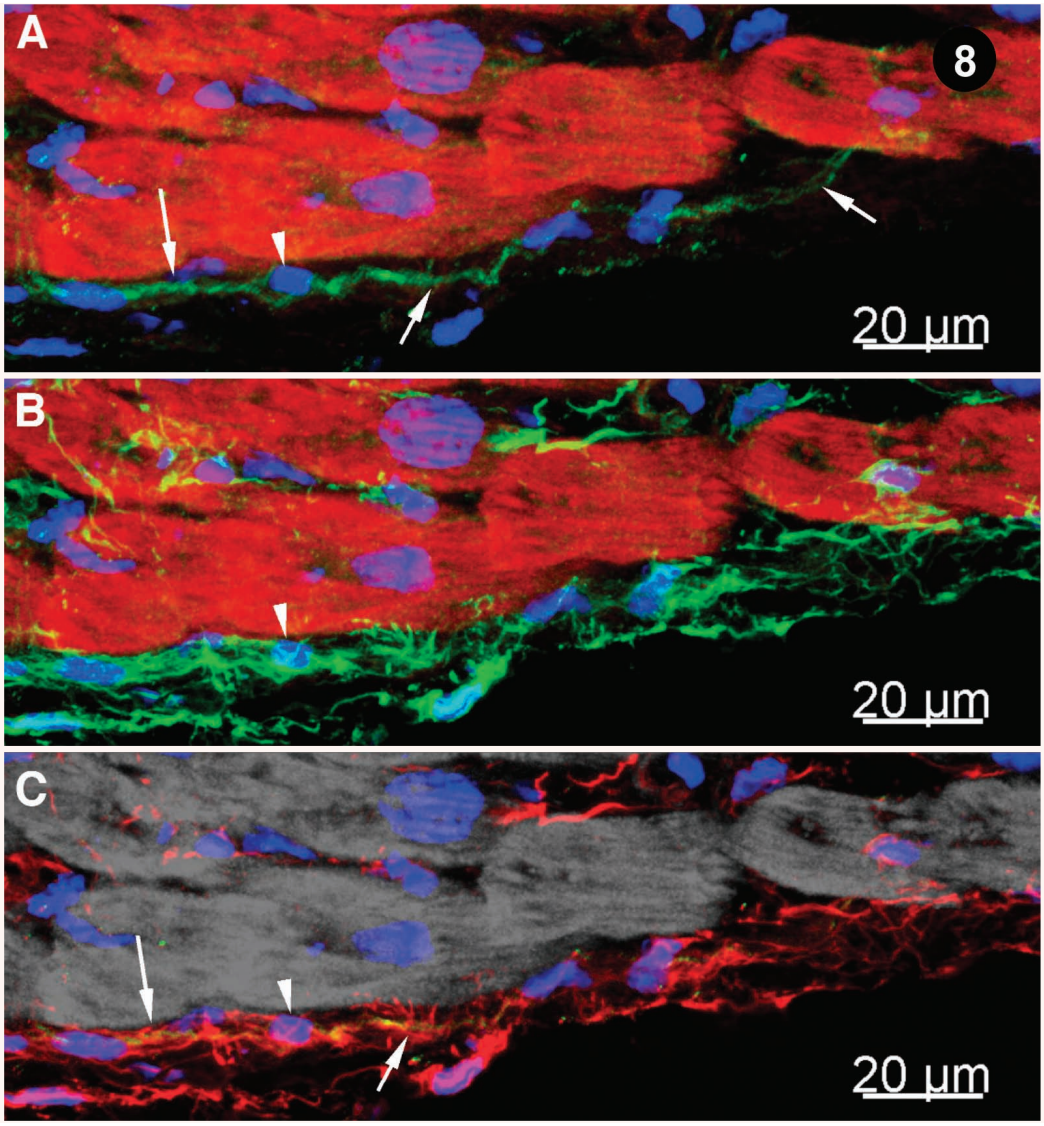

Fig. 8 Immunohistochemistry of human left ventricle myocardium; CLSM.
(**A**) CD117/c-kit$^+$ cells (green) with long cytoplasmic processes (indicated by arrows) indicated by arrows; myofibrils are stained bright-red with Alexa 633-phalloidin and nuclei are stained blue with DAPI. The arrowhead shows the nucleus of a c-kit$^+$ cell.
(**B**) Vimentin positive cells (green); myofibrils appear bright red, stained with Alexa 633-phalloidin and nuclei blue with DAPI (arrowhead).
(**C**) Merged view of images (**A**) and (**B**) showing that c-kit signal (green) co-localizes with vimentin (red) resulting a yellow colour (arrows). Note that most of cells are only vimentin positive (red) and only a few are positive for both c-kit and vimentin. Myofibrils are pseudo-coloured in grey. The arrowhead indicates a nucleus (blue).

Figure 8 shows the images obtained by CLSM concerning the existence of c-kit$^+$ (Fig. 8A) or vimentin (Fig. 8B) cells in human left ventricle myocardium. However, Fig. 8C indicates that only a few cells (three to four) appear positive for both c-kit and vimentin, concomitantly. This confirms again our previous report about c-kit immunopositivity in rat ventricle [10].

Figure 9 shows a typical bipolar ICLCs in the narrow space between three cardyomyocites. At least 24 shedding microvesicles (red arrows) budding from the plasma membrane of ICLCs are clearly visible. Such vesicles of about 200–400 nm were considered for a long time to be artefacts, but now are recognized as specific leptostructures that are distinct from the exosomes released upon exocytosis of multivesicular bodies [48–50]. Exosomes have diameters of only 30–100 nm [48]. Anyway, shedding microvesicles like those shown in Fig. 9 are no longer artefacts or 'little more than garbage bags', containing materials that cell needed to get rid of [48, 50].

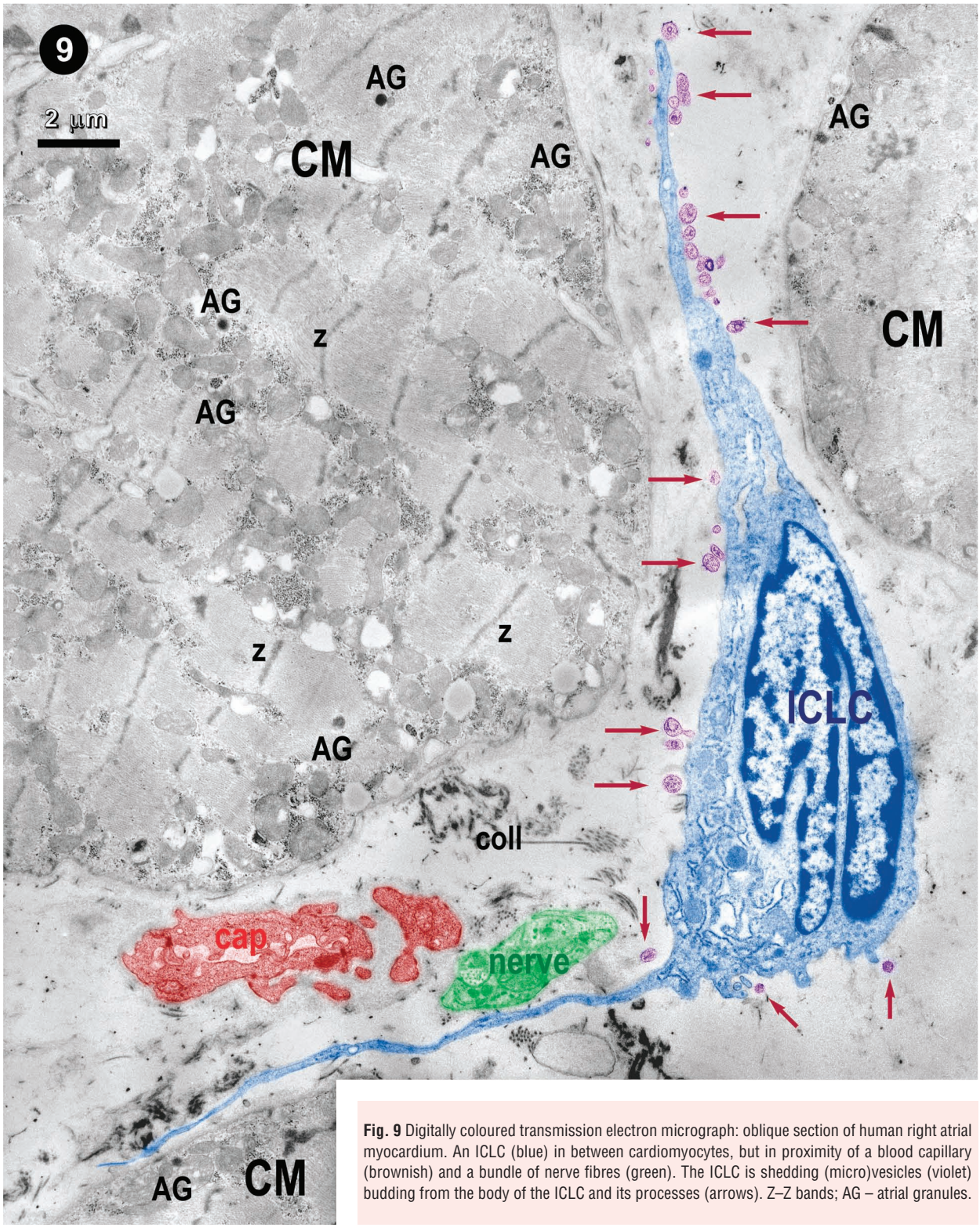

Fig. 9 Digitally coloured transmission electron micrograph: oblique section of human right atrial myocardium. An ICLC (blue) in between cardiomyocytes, but in proximity of a blood capillary (brownish) and a bundle of nerve fibres (green). The ICLC is shedding (micro)vesicles (violet) budding from the body of the ICLC and its processes (arrows). Z–Z bands; AG – atrial granules.

Table 1 Comparative characteristics of ICC, ICLCs and fibroblasts

		INTERSTITIAL CELLS OF CAJAL (ICC) digestive tract, see refs. 38, 51, 54	INTERSTITIAL CAJAL-LIKE CELLS (ICLC) digestive tract [38, 54], detrusor [22] and myocardium [9, 10, 40, 41–43] and present results	FIBROBLASTS *(IN SITU)* see [53, 54]
Number		Depends on the anatomic region (less in colon versus small bowel)	~2% of atrial myocardium volume ~1% of ventricular myocardium volume	Large majority of cells in the nonmyocytic space (~50% atrial volume and ~30% of ventricular volume)
General aspect		Spindle-shaped and large-sized cells Oval body, containing the nucleus and a large quantity of cytoplasm	Piriform or spindle or triangular or stellate body containing the nucleus and a small quantity of cytoplasm	Pleiomorphic (phenotypic heterogeneity) cell body contains the nucleus and a large quantity of cytoplasm
Nucleus/chromatin		Oval, euchromatin	Oval, hetero- and eu-chromatin	Oval, mostly euchromatin
Organelle	**Mito**	Many, distributed everywhere in cytoplasm	Occupy 5–10% of cell volume, several in the perinuclear cytoplasm and typically in the dilations (knobs) of the cytoplasmic processes	Several
	Golgi	Medium sized	Small	Prominent
	ER	Extended smooth ER and few cisternae of rough ER	Smooth ER <1% of cell volume, and several cisternae of rough ER (~1–2%). ER is also located inside the cell processes at the level of their dilations (knobs)	Smooth ER absent, but rough ER prominent (8–12% of cell volume)
Cell processes	**Number**	>2	2–5	Usually 2
	Length	Variable (micrometers)	Extremely long (tens up to hundred of micrometers)	Short (micrometers)
	Thickness and Emergence	Thick at the starting point from the cell body, gradual thinning	Very thin (~0.2–0.4 mm). Thin, suddenly, at the starting point from the cell body. Uneven calibre with specific moniliform aspect: dilations (knobs) alternating with thin narrow segments	Thick emergence followed by gradual thinning
	Profile	Intermingling	Labyrinthic	Triangular
	Ramifications	Several	Many, dichotomic pattern	Unexplored
Cytoskeleton filaments		Cytoskeleton filaments	Thin and intermediate	Intermediate
Caveolae		Many	Many (~2% of cytoplasmic volume)	Virtually absent *
Ca^{2+} handling units		Unexplored	Composed of caveolae, ER and mitochondria Present within the dilations (knobs) of cell processes	Unexplored
Shedding microvesicles		Unexplored	Present	Unexplored
Basal lamina		Discontinuous	Inconstant	No basal lamina
Specific markers		c-kit (possible co-localization with CD 34)	CD34, (inconstant co-localization of c-kit)	No specific marker; positive for vimentin, DDR2
Close Contacts		Gap junctions to each other and/with smooth muscle cells and nerve endings	Gap-like junctions to each other and with smooth muscle cells; frequent Close vicinity with nerve endings and capillary 'Stromal synapses' with connective cells and immunoreactive cells	No close contacts with different cells
Proliferative potential		Age-dependent ? **	(Adult) mesenchymal stem cells ? Uncommitted progenitor cells ? Cardiac repair/regeneration ?	Significantly responsible for remodelling and fibrosis

*Fibroblasts *in situ* have no caveolae [10, 22, 39, 40, 55]. Although several authors claimed that fibroblasts have caveolae, in fact caveolae could be found in human or mammalian fibroblasts, but **only *in vitro***, in cultured cells, when the phenotype is changed.
**See [56]

Shedding vesicles could participate in important biological processes and their significant number at the surface of an ICLC *in situ* (Fig. 9) suggests that these lepto-structures may transport, as cargo, important information to other cells over nano(micro) distances.

Discussion

Table 1 shortens the 'Discussion' and clearly shows that the ICLCs of human or mammalian myocardium represent a distinct cell type, different from classical (intestinal) ICC or fibroblasts. Moreover, a comparison of ICLCs with myofibroblasts is not necessary since myofibroblasts do not exist in healthy tissues [57].

It should be noted that, at present, although the ICLC existence as a distinct cell population is unequivocal, the (exact) functions of ICLCs in myocardium are unknown. Therefore, it seems attractive to enumerate several possibilities:

(1) ICLCs are involved in intercellular signalling since they have a strategic position, very closed to cardiomyocytes, blood capillaries and nerve endings and, in addition, ICLCs form a 3D-network (Fig. 5). At least two mechanisms could be considered: (*i*) a paracrine and/or juxtacrine secretion of small signal molecules and (*ii*) shedding microvesicles (see Fig. 9), which play unique roles in the 'horizontal' transfer of important macromolecules (*e.g.* proteins or RNAs) among neighbouring cells, necessary for the rapid phenotype adjustments in a variety of conditions [50].

(2) ICLCs seem to be mechanoreceptors/transducers as previously discussed [40, 42]. This is mainly suggested by their extremely long cytoplasmic processes (tens up to hundreds micrometers; see Figs. 1, 3, 6 and 9). It is noteworthy, considering the microscopic anatomy or histology, that only some specialized nerve cells have cell processes longer than ICLCs (the length does matter!).

(3) ICLCs could participate in pacemaking and/or arrhythmogenesis. For instance, very recently we described a significant population of ICLCs in myocardial sleeves of pulmonary veins [42] and another group found c-kit$^+$ cells in similar locations [37]. Although, the mechanisms of atrial fibrilation are still the subject of controversies [58], many authors favour 'the pulmonary vein wave' hypothesis [59–63]. Indeed, Anderson [64], wrote: 'Precise knowledge of the source of the abnormal rhythms originating within the pulmonary veins would contribute immensely to clarifying our understanding of this vexatious arrhythmia'.

(4) In myocardium, ICLCs might be considered as adult stromal mesenchymal stem cells. ICLCs might also be viewed as an unexplored population of uncommitted c-kit$^+$ resident cells [65]. Undeniably, the identification of cardiac progenitor/stem cells (sometimes c-kit$^+$) is currently a hot subject [66–72]. If ICLCs are progenitor/stem cells in myocardium, then the variable c-kit positivity (Table 1) may reflect different functional/pathological circumstances. Naturally, ICLCs could be a therapeutic target for regenerative cardiovascular medicine [65, 73–75].

In conclusion, instead of believing that fibroblasts are perhaps the most underestimated cell population in the heart [53], we suggest that ICLCs are really neglected, although they might be key players in understanding cardiac (ultra-)structure–function relationships.

References

1. **Rumessen JJ, Vanderwinden JM.** Interstitial cells in the musculature of the gastrointestinal tract: Cajal and beyond. *Int Rev Cytol.* 2003; 229: 115–208.
2. **Faussone-Pellegrini MS.** Interstitial cells of Cajal: once negligible players, now blazing protagonists. *Ital J Anat Embryol.* 2005; 110: 11–31.
3. **Sanders KM, Koh SD, Ward SM.** Interstitial cells of Cajal as pacemakers in the gastrointestinal tract. *Annu Rev Physiol.* 2006; 68: 307–43.
4. **Nakayama S, Kajioka S, Goto K, Takaki M, Liu HN.** Calcium-associated mechanisms in gut pacemaker activity. *J Cell Mol Med.* 2007; 11: 958–68.
5. **Yin J, Chen JD.** Roles of interstitial cells of Cajal in regulating gastrointestinal motility: *in vitro versus in vivo* studies. *J Cell Mol Med.* 2008; 12: 1118–29.
6. **Farrugia G.** Interstitial cells of Cajal in health and disease. *Neurogastroenterol Motil.* 2008; 20: 54–63.
7. **Huizinga JD, Faussone-Pellegrini MS.** About the presence of interstitial cells of Cajal outside the musculature of the gastrointestinal tract. *J Cell Mol Med.* 2005; 9: 468–73.
8. **Gherghiceanu M, Popescu LM.** Interstitial Cajal-like cells (ICLC) in human resting mammary gland stroma. Transmission electron microscope (TEM) identification. *J Cell Mol Med.* 2005; 9: 893–910.
9. **Hinescu ME, Popescu LM.** Interstitial Cajal-like cells (ICLC) in human atrial myocardium. *J Cell Mol Med.* 2005; 9: 972–5.
10. **Popescu LM, Gherghiceanu M, Hinescu ME, Cretoiu D, Ceafalan L, Regalia T, Popescu AC, Ardeleanu C, Mandache E.** Insights into the interstitium of ventricular myocardium: interstitial Cajal-like cells (ICLC). *J Cell Mol Med.* 2006; 10: 429–58.
11. **Popescu LM, Ciontea SM, Cretoiu D.** Interstitial Cajal-like cells in human uterus and fallopian tube. *Ann NY Acad Sci.* 2007; 1101: 139–65.
12. **Popescu LM, Hinescu ME, Ionescu N, Ciontea SM, Cretoiu D, Ardelean C.** Interstitial cells of Cajal in pancreas. *J Cell Mol Med.* 2005; 9: 169–90.
13. **Hinescu ME, Ardeleanu C, Gherghiceanu M, Popescu LM.** Interstitial Cajal-like cells in human gallbladder. *J Mol Histol.* 2007; 38: 275–84.
14. **Lavoie B, Balemba OB, Nelson MT, Ward SM, Mawe GM.** Morphological and physiological evidence for interstitial cell of Cajal-like cells in the guinea pig gallbladder. *J Physiol.* 2007; 579: 487–501.
15. **Balemba OB, Bartoo AC, Nelson MT, Mawe GM.** Role of mitochondria in spontaneous rhythmic activity and intracellular calcium waves in the guinea pig gallbladder smooth muscle. *Am J Physiol Gastrointest Liver Physiol.* 2008; 294: G467–76.
16. **Lang RJ, Klemm MF.** Interstitial cell of Cajal-like cells in the upper urinary tract. *J Cell Mol Med.* 2005; 9: 543–56.
17. **McHale NG, Hollywood MA, Sergeant GP, Shafei M, Thornbury KT, Ward SM.**

Organization and function of ICC in the urinary tract. *J Physiol.* 2006; 576: 689–94.

18. **Hashitani H.** Interaction between interstitial cells and smooth muscles in the lower urinary tract and penis. *J Physiol.* 2006; 576: 707–14.
19. **Lang RJ, Zoltkowski BZ, Hammer JM, Meeker WF, Wendt I.** Electrical characterization of interstitial cells of Cajal-like cells and smooth muscle cells isolated from the mouse ureteropelvic junction. *J Urol.* 2007; 177: 1573–80.
20. **Rasmussen H, Hansen A, Smedts F, Rumessen JJ, Horn T.** CD34-positive interstitial cells of the human detrusor. *APMIS.* 2007; 115: 1260–6.
21. **Metzger R, Neugebauer A, Rolle U, Böhlig L, Till H.** C-Kit receptor (CD117) in the porcine urinary tract. *Pediatr Surg Int.* 2008; 24: 67–76.
22. **Rasmussen H, Rumessen JJ, Hansen A, Smedts F, Horn T.** Ultrastructure of Cajal-like interstitial cells in the human detrusor. *Cell Tissue Res.* 2009; 10.1007/s00441–008-0736-z.
23. **Ciontea SM, Radu E, Regalia T, Ceafalan L, Cretoiu D, Gherghiceanu M, Braga RI, Malincenco M, Zagrean L, Hinescu ME, Popescu LM.** C-kit immunopositive interstitial cells (Cajal-type) in human myometrium. *J Cell Mol Med.* 2005; 9: 407–20.
24. **Popescu LM, Vidulescu C, Curici A, Caravia L, Simionescu AA, Ciontea SM, Simion S.** Imatinib inhibits spontaneous rhythmic contractions of human uterus and intestine. *Eur J Pharmacol.* 2006; 546: 177–81.
25. **Hutchings G, Deprest J, Nilius B, Roskams T, De Ridder D.** The effect of imatinib mesylate on the contractility of isolated rabbit myometrial strips. *Gynecol Obstet Invest.* 2006; 62: 79–83.
26. **Allix S, Reyes-Gomez E, Aubin-Houzelstein G, Noël D, Tiret L, Panthier JJ, Bernex F.** Uterine contractions depend on KIT-positive interstitial cells in the mouse: genetic and pharmacological evidence. *Biol Reprod.* 2008; 79: 510–7.
27. **Hutchings G, Gevaert T, Deprest J, Roskams T, Van Lommel A, Nilius B, De Ridder D.** Immunohistochemistry using an antibody to unphosphorylated connexin 43 to identify human myometrial interstitial cells. *Reprod Biol Endocrinol.* 2008; 6: 43–50.
28. **Terada T.** Gastrointestinal stromal tumor of the uterus: a case report with genetic analyses of c-kit and PDGFRA genes. *Int J Gynecol Pathol.* 2009; 28: 29–34.
29. **Popescu LM, Ciontea SM, Cretoiu D, Hinescu ME, Radu E, Ionescu N, Ceausu M, Gherghiceanu M, Braga RI, Vasilescu F, Zagrean L, Ardeleanu C.** Novel type of interstitial cell (Cajal-like) in human fallopian tube. *J Cell Mol Med.* 2005; 9: 479–523.
30. **Dixon RE, Hwang SJ, Hennig GW, Ramsey KH, Schripsema JH, Sanders KM, Ward SM.** Chlamydia infection causes loss of pacemaker cells and inhibits oocyte transport in the mouse oviduct. *Biol Reprod.* 2009 Jan 7. DOI: 10.1095/biolreprod.108.073833.
31. **Suciu L, Popescu LM, Gherghiceanu M.** Human placenta: *de visu* demonstration of interstitial Cajal-like cells. *J Cell Mol Med.* 2007; 11: 590–7.
32. **Shafik A, Shafik I, el-Sibai O.** Identification of c-kit-positive cells in the human prostate: the interstitial cells of Cajal. *Arch Androl.* 2005; 51: 345–51.
33. **Hinescu ME, Popescu LM, Gherghiceanu M, Faussone-Pellegrini MS.** Interstitial Cajal-like cells in rat mesentery: an ultrastructural and immunohistochemical approach. *J Cell Mol Med.* 2008; 12: 260–70.
34. **Harhun M, Gordienko D, Kryshtal D, Pucovský V, Bolton T.** Role of intracellular stores in the regulation of rhythmical $[Ca^{2+}]$I changes in interstitial cells of Cajal from rabbit portal vein. *Cell Calcium.* 2006; 40: 287–98.
35. **Pucovský V, Harhun MI, Povstyan OV, Gordienko DV, Moss RF, Bolton TB.** Close relation of arterial ICC-like cells to the contractile phenotype of vascular smooth muscle cell. *J Cell Mol Med.* 2007; 11: 764–75.
36. **Bobryshev YV.** Subset of cells immunopositive for neurokinin-1 receptor identified as arterial interstitial cells of Cajal in human large arteries. *Cell Tissue Res.* 2005; 321: 45–55.
37. **Morel E, Meyronet D, Thivolet-Bejuy F, Chevalier P.** Identification and distribution of interstitial Cajal cells in human pulmonary veins. *Heart Rhythm.* 2008; 5: 1063–7.
38. **McCloskey KD, Hollywood MA, Thornbury KD, Ward SM, McHale NG.** Kit-like immunopositive cells in sheep mesenteric lymphatic vessels. *Cell Tissue Res.* 2002; 310: 77–84.
39. **Pieri L, Vannucchi MG, Faussone-Pellegrini MS.** Histochemical and ultrastructural characteristics of an interstitial cell type different from ICC and resident in the muscle coat of human gut. *J Cell Mol Med.* 2008; 12: 1944–55.
40. **Hinescu ME, Gherghiceanu M, Mandache E, Ciontea SM, Popescu LM.** Interstitial Cajal-like cells (ICLC) in atrial myocardium: ultrastructural and immunohistochemical characterization. *J Cell Mol Med.* 2006; 10: 243–57.
41. **Mandache E, Popescu LM, Gherghiceanu M.** Myocardial interstitial Cajal-like cells (ICLC) and their nanostructural relationships with intercalated discs: shed vesicles as intermediates. *J Cell Mol Med.* 2007; 11: 1175–84.
42. **Gherghiceanu M, Hinescu ME, Andrei F, Mandache E, Macarie CE, Faussone-Pellegrini MS, Popescu LM.** Interstitial Cajal-like cells (ICLC) in myocardial sleeves of human pulmonary veins. *J Cell Mol Med.* 2008; 12: 1777–81.
43. **Gherghiceanu M, ME Hinescu, LM Popescu.** Myocardial interstitial Cajal-like cells (ICLC) in caveolin-1 KO mice. *J Cell Mol Med.* 2009; 13: 201–5.
44. **Miyamoto T, Zhang L, Sekiguchi A, Hadama T, Shimada T.** Structural differences in the cytoarchitecture and intercalated discs between the working myocardium and conduction system in the human heart. *Heart Vessels.* 2002; 16: 232–40.
45. **Kostin S, Scholz D, Shimada T, Maeno Y, Mollnau H, Hein S, Schaper J.** The internal and external protein scaffold of the T-tubular system in cardiomyocytes. *Cell Tissue Res.* 1998; 294: 449–60.
46. **Kostin S, Schaper J.** Tissue-specific patterns of gap junctions in adult rat atrial and ventricular cardiomyocytes *in vivo* and *in vitro*. *Circ Res.* 2001; 88: 933–9.
47. **Kostin S.** Zonula occludens-1 and connexin 43 expression in the failing human heart. *J Cell Mol Med.* 2007; 11: 892–5.
48. **Lakkaraju A, Rodriguez-Boulan E.** Itinerant exosomes: emerging roles in cell and tissue polarity. *Trends Cell Biol.* 2008; 18: 199–209.
49. **Spang A.** The life cycle of a transport vesicle. *Cell Mol Life Sci.* 2008; 65: 2781–9.
50. **Cocucci E, Racchetti G, Meldolesi J.** Shedding microvesicles: artefacts no more. *Trends Cell Biol.* 2009; doi: 10.1016/j.tcb.2008.11.003.
51. **Faussone-Pellegrini MS, Thuneberg L.** Guide to the identification of interstitial cells of Cajal. *Microsc Res Tech.* 1999; 47: 248–66.
52. **Junquera C, Marténez-Ciriano C, Castiella T, Serrano P, Azanza MJ, Junquera SR.** Immunohistochemical and ultrastructural characteristics of interstitial cells of Cajal in the rabbit duodenum. Presence of a single cilium. *J Cell Mol Med.* 2007; 11: 776–87.
53. **Goldsmith EC, Hoffman A, Morales MO, Potts JD, Price RL, McFadden A, Rice M,**

Borg TK. Organization of fibroblasts in the heart. *Dev Dyn.* 2004 Aug; 230: 787–94.
54. **Camelliti P, Green CR, Kohl P**. Structural and functional coupling of cardiac myocytes and fibroblasts. *Adv Cardiol.* 2006; 42: 132–49.
55. **Schurch W, Seemayer TA, Gabbiani G.** The myofibroblast: In: Sternberg SS, editor. Histology for pathologists. 2nd ed. Philadelphia: Lippincott-Raven; 1997. pp. 129–65.
56. **Mei F, Zhu J, Guo S, Zhou DS, Han J, Yu B, Li SF, Jiang ZY, Xiong CJ.** An age-dependent proliferation is involved in the postnatal development of interstitial cells of Cajal in the small intestine of mice. *Histochem Cell Biol.* 2009; 131: 43–53.
57. **Eyden B.** The myofibroblast: phenotypic characterization as a prerequisite to understanding its functions in translational medicine. *J Cell Mol Med.* 2008; 12: 22–37.
58. **Nattel S, Opie LH.** Controversies in atrial fibrillation. *Lancet.* 2006; 367: 262–72.
59. **Haissaguerre M, Sanders P, Hocini M, Jais P, Clémenty J.** Pulmonary veins in the substrate for atrial fibrillation: the "venous wave" hypothesis. *J Am Coll Cardiol.* 2004; 43: 2290–2.
60. **Huang CX, Hu CL, Li YB.** Atrial fibrillation may be a vascular disease: the role of the pulmonary vein. *Med Hypotheses.* 2007; 68: 629–34.
61. **Noheria A, Kumar A, Wylie JV Jr, Josephson ME.** Catheter ablation *vs.* antiarrhythmic drug therapy for atrial fibrillation: a systematic review. *Arch Intern Med.* 2008; 168: 581–6.
62. **Rostock T, Steven D, Lutomsky B, Servatius H, Drewitz I, Klemm H, Müllerleile K, Ventura R, Meinertz T, Willems S.** Atrial fibrillation begets atrial fibrillation in the pulmonary veins on the impact of atrial fibrillation on the electrophysiological properties of the pulmonary veins in humans. *J Am Coll Cardiol.* 2008; 51: 2153–60.
63. **Seol CA, Kim WT, Ha JM, Choe H, Jang YJ, Youm JB, Earm YE, Leem CH.** Stretchactivated currents in cardiomyocytes isolated from rabbit pulmonary veins. *Prog Biophys Mol Biol.* 2008; 97: 217–31.
64. **Anderson RH.** The anatomic substrates for abnormal automaticity in the pulmonary veins. *Heart Rhythm.* 2008; 5: 1068–9.
65. **Nesselmann C, Ma N, Bieback K, Wagner W, Ho A, Konttinen YT, Zhang H, Hinescu ME, Steinhoff G.** Mesenchymal stem cells and cardiac repair. *J Cell Mol Med.* 2008; 12: 1795–810.
66. **Ayach BB, Yoshimitsu M, Dawood F, Sun M, Arab S, Chen M, Higuchi K, Siatskas C, Lee P, Lim H, Zhang J, Cukerman E, Stanford WL, Medin JA, Liu PP.** Stem cell factor receptor induces progenitor and natural killer cell-mediated cardiac survival and repair after myocardial infarction. *Proc Natl Acad Sci USA.* 2006; 103: 2304–9.
67. **Anversa P, Kajstura J, Leri A, Bolli R.** Life and death of cardiac stem cells: a paradigm shift in cardiac biology. *Circulation.* 2006; 21; 113: 1451–63.
68. **Cimini M, Fazel S, Zhuo S, Xaymardan M, Fujii H, Weisel RD, Li RK.** c-kit dysfunction impairs myocardial healing after infarction. *Circulation.* 2007; 116: I77–82.
69. **Ott HC, Matthiesen TS, Brechtken J, Grindle S, Goh SK, Nelson W, Taylor DA.** The adult human heart as a source for stem cells: repair strategies with embryonic-like progenitor cells. *Nat Clin Pract Cardiovasc Med.* 2007; 4: S27–39.
70. **Barile L, Chimenti I, Gaetani R, Forte E, Miraldi F, Frati G, Messina E, Giacomello A.** Cardiac stem cells: isolation, expansion and experimental use for myocardial regeneration. *Nat Clin Pract Cardiovasc Med.* 2007; 4: S9–S14.
71. **Wu SM, Chien KR, Mummery C.** Origins and fates of cardiovascular progenitor cells. *Cell.* 2008; 132: 537–43.
72. **Martin-Puig S, Wang Z, Chien KR.** Lives of a heart cell: tracing the origins of cardiac progenitors. *Cell Stem Cell.* 2008; 2: 320–31.
73. **Mazhari R, Hare JM.** Mechanisms of action of mesenchymal stem cells in cardiac repair: potential influences on the cardiac stem cell niche. *Nat Clin Pract Cardiovasc Med.* 2007; 4: S21–6.
74. **Chien KR.** Regenerative medicine and human models of human disease. *Nature.* 2008; 453: 302–5.
75. **Chien KR, Domian IJ, Parker KK.** Cardiogenesis and the complex biology of regenerative cardiovascular medicine. *Science.* 2008; 322: 1494–7.